SIZE AS A LINE OF LEAST EVOLUTIONARY RESISTANCE: DIET AND ADAPTIVE MORPHOLOGICAL RADIATION IN NEW WORLD MONKEYS

GABRIEL MARROIG[1,2] AND JAMES M. CHEVERUD[3,4]

[1]*Departamento de Genética e Biologia Evolutiva, Instituto de Biociências, Universidade de São Paulo, CP 11.461, CEP 05422-970, São Paulo, SP, Brazil*
[2]*E-mail: gmarroig@ib.usp.br*
[3]*Department of Anatomy and Neurobiology, Washington University School of Medicine, 660 South Euclid Avenue, Campus Box 8108, Saint Louis, Missouri, 63110*
[4]*E-mail: cheverud@pcg.wustl.edu*

Abstract.—New World monkeys (NWM) display substantial variation (two orders of magnitude) in body size. Despite this, variation in skull size and associated shape show a conserved allometric relationship, both within and between genera. Maximum likelihood estimates of quantitative ancestral states were used to compare the direction of morphological differentiation with the phenotypic ($\mathbf{p_{max}}$) and genetic ($\mathbf{g_{max}}$) lines of least evolutionary resistance (LLER). Diversification in NWM skulls occurred principally along the LLER defined by size variation. We also obtained measures of morphological amount and pace of change using our skull data together with published genetic distances to test whether the LLER influenced the amount and pace of diversification. Moreover, data on an ecological factor (diet) was obtained from the literature and used to test the association of this niche-related measure with the morphological diversification. Two strategies were used to test the association of LLER with the morphological and dietary amount and pace of change, one focusing on both contemporary genera and maximum likelihood reconstructed ancestors and the other using only the 16 contemporary genera in a phylogenetic comparative analysis. Our results suggest that the LLER influenced the path, amount, and pace of morphological change. Evolution also occurred away from the LLER in some taxa but this occurred at a slower pace and resulted in a relatively low amount of morphological change. We found that longer branch lengths (time) are associated with larger differences in $\mathbf{p_{max}}$ orientation. However, on a macroevolutionary scale there is no such trend. Diet is consistently associated with both absolute size differences and morphological integration patterns, and we suggest that this ecological factor might be driving adaptive radiation in NWM. Invasion of diet-based adaptive zones involves changes in absolute size, due to metabolic and foraging constraints, resulting in simple allometric skull diversification along the LLER. While it is clear that evolutionary change occurred along the LLER, it is not clear whether this macroevolutionary pattern results from a conservation of within-population genetic covariance patterns or long-term adaptation along a size dimension or whether both constraints and selection were inextricably involved.

Key words.—Adaptation, allometry, constraints, evolutionary processes, morphological evolution, Platyrrhini, quantitative genetics.

Received May 26, 2004. Accepted February 16, 2005.

Patterns of genetic and developmental variation might constrain or facilitate the evolution of morphological complexes and direct the pathways and pace of evolutionary change. While constraints sometimes are perceived as an obstacle to evolution in some directions, they might also be envisaged as facilitating the adaptive process along what Schluter (1996) called ''genetic lines of least evolutionary resistance.'' Several questions can be asked about those lines of least evolutionary resistance (LLER): Do they exist? For how long do they persist through time? How much diversification can occur along such lines? Do they exert a strong influence on the path of evolutionary change? Here, we follow Schluter (1996) and refer specifically to a single simple factor: the multivariate direction of greatest genetic (or its phenotypic surrogate) variation ($\mathbf{g_{max}}$ or $\mathbf{p_{max}}$). This factor is a linear combination of a suite of morphological traits that displays the maximum within-population variance. It defines a LLER to evolutionary change by either natural selection or genetic drift (Arnold et al. 2001). Schluter (1996) suggested that most evolutionary diversification may occur along these lines of least resistance. Here we use the New World monkeys (NWM) as a model to test some ideas related to the lines of least resistance and adaptive evolution. In particular, three predictions stemming from the LLER model (Schluter 1996) are tested. The first is that populations recently diverged from

a common ancestor should differ along a dimension defined by $\mathbf{g_{max}}$. The second is that this bias in the direction of evolution should be temporary and diminish with time. The third prediction is that evolutionary change should be relatively slow if selection favors divergence in a direction markedly different from that of $\mathbf{g_{max}}$, unless $\mathbf{g_{max}}$ itself evolves during divergence.

NWM are anthropoid primates of the infraorder Platyrrhini, the sister group of the Old World monkeys (Catarrhini), which also includes apes and humans. The evolutionary diversification of NWM occurred over a period of more than 30 million years (at least since the Oligocene). They are taxonomically diverse, including at least 110 species (Rylands et al. 2000), and show substantial variation in body size, ranging over two orders of magnitude from the smallest pygmy marmoset (*Cebuella*) to the woolly spider monkey (*Brachyteles*; Hershkovitz 1977; Fleagle 1999). Platyrhines (NWM) are primarily diurnal (except the night monkeys *Aotus*) and arboreal, living in tropical and subtropical forests ranging from Mexico to Argentina. While primarily forest inhabitants, NWM live in a variety of forest types, feeding on several types of animal and vegetal items and have complex and distinctive mating systems (Coimbra-Filho and Mittermeier 1981; Mittermeier et al. 1988; Norconk et al. 1996; Kinsey 1997). These differences in habitats, habits, and life

histories are reflected in their distinct morphologies, with changes in size and shape of the body and in particular in the cranium (see Hershkovitz 1977). NWM are relatively stable taxonomically at the generic level (Schneider and Rosenberger 1996; Marroig and Cheverud 2001; Schneider et al. 2001) and phylogenetic relationships among them are well resolved. Molecular data are available (Schneider 2000; Schneider et al. 2001), allowing morphological evolution to be studied in the context of historical patterns of ancestry.

Previously, we showed that phenotypic variance/covariance patterns in the skull of NWM are remarkably stable and that minor variations in those patterns are associated with dietary differences but not phylogeny (Marroig and Cheverud 2001). Also, we showed that morphological diversification in NWM was dominated by natural selection and suggested that the adaptive radiation of these primates was triggered by an association of size evolution and diet diversification (Marroig and Cheverud 2004). All these previous studies and detailed information about phylogeny and ecology in NWM make them an ideal taxon for a quantitative evolutionary investigation of their adaptive radiation. Here we present an analysis of cranial size and allometric shape variation in NWM. In addition, we compare the direction of evolution (Δz or the vector of average differences for a suite of morphological traits) with the LLER (g_{max} and p_{max}), mapping the correlation of Δz-g_{max} and Δz-p_{max} along the NWM phylogeny. We also explore the association of an ecological factor (diet), with size, time, LLER and the amount and pace of evolutionary change, structuring our comparisons within a phylogenetic context.

MATERIALS AND METHODS

Sample, Measurements, and Repeatability

Skull measurements were obtained from 5222 crania of 16 genera and 110 species of Platyrrhini deposited at the following institutions: American Museum of Natural History, British Museum of Natural History, Field Museum of Natural History, Museu de Zoologia da Universidade de São Paulo, Museu Nacional do Rio de Janeiro, Museu Paranaense Emílio Goeldi, Museo de la Universidad Nacional Mayor de San Marcos, National Museum of Natural History, and the University of Tennessee, derived from the Marmoset Research Center, Oak Ridge Associated Universities' colonies. A complete list of examined specimens may be obtained from the authors upon request, and details of the taxonomic arrangement employed and sample sizes for each taxon are given in Marroig and Cheverud (2001). Only adult crania were used in the subsequent analyses. Specimens were considered adult when they had totally erupted and functional dentition as well as closed or fused spheno-occipital and/or spheno-ethmoid sutures.

Three-dimensional coordinates were recorded for 36 landmarks (Fig. 1) using a Polhemus 3Draw digitizer (Colchester, VT). The general procedure for measuring specimens and the landmark definitions follow Cheverud (1995). A set of 70 linear measurements describing cranial morphology was calculated from the coordinate values. This set was reduced to 39 measurements, averaging the measurements present on both sides of the skull (for the list of 39 traits see Marroig

and Cheverud 2001, 2004). Repeatabilities for our measurements are generally above 0.90 when considering variation within a single population (Cheverud 1995, 1996; Ackermann and Cheverud 2000; Marroig and Cheverud 2001).

Overall Strategy, Summary, and Symbols

Tables 1 and 2 present a summary of the symbols used for the variables and analyses performed. Most analyses described below are based on the comparative method and make use of the NWM phylogeny to reconstruct ancestral estimates for each node in the tree. Thus, the overall strategy is to focus on phylogenetically independent changes and associations occurring within each internode (along branches) of the tree. In addition, we use a more familiar method to test for association among our variables using the independent contrasts (IC) to account for the nonindependence of phylogenetically structured data (Garland and Ives 2000). We use the module PDAP (Garland and Ives 2000) within the Mesquite package (Maddison and Maddison 2003) to obtain the correlation among variables under the IC approach.

Size Vector, Line of Least Resistance, and the Direction of Evolution

Pooled within-group phenotypic variance/covariance matrices (below referred to as covariance matrices or W for simplicity) were estimated for each genus using the general linear model (GLM) SYSTAT 11.0 (Systat Software, Inc., Richmond, CA) routine to control for sexual dimorphism and species differences whenever appropriate (for details see Marroig and Cheverud 2001). Averages for the 16 genera were obtained as least squares averages from the GLM module in SYSTAT with genera and species nested within genera as independent factors and the skull trait set ($n = 39$) as dependent variables. Throughout the paper we use vector correlation to measure the similarity of any two vectors. The vector correlation (Blackith and Reyment 1971) is a measure of vector orientation similarity in a p-dimensional space (p being the number of traits). The correlation between two vectors is equal to the cosine of the angle θ formed between them. The expected range of correlations commonly occurring among 39-element vectors by chance alone is $-0.4 < r < 0.4$ (Ackermann and Cheverud 2000), but only absolute values need to be taken into consideration because an angle of $\theta > 90°$ is equivalent to one of $180° - \theta$. We use a broken-stick model to obtain 1000 random 39-element vectors from a uniform distribution to then correlate each random vector to a fixed isometric vector (all elements equal 0.160). Our sample showed an average correlation of 0.127 and a SD of 0.095, both values being the same no matter which fixed vector was used for comparisons with the random vectors. These two statistics, based on a random sample of 39-element vectors, allow us to test whether the correlation of any two observed vectors is significantly different from the correlation between two vectors expected by chance.

Similarity in the p_{max} direction might be an indication of a shared LLER, but that does not mean that evolution necessarily follows that path. To test whether the LLER influenced the direction of morphological diversification, we need to compare the orientation of g_{max} to Δz. We first estimate
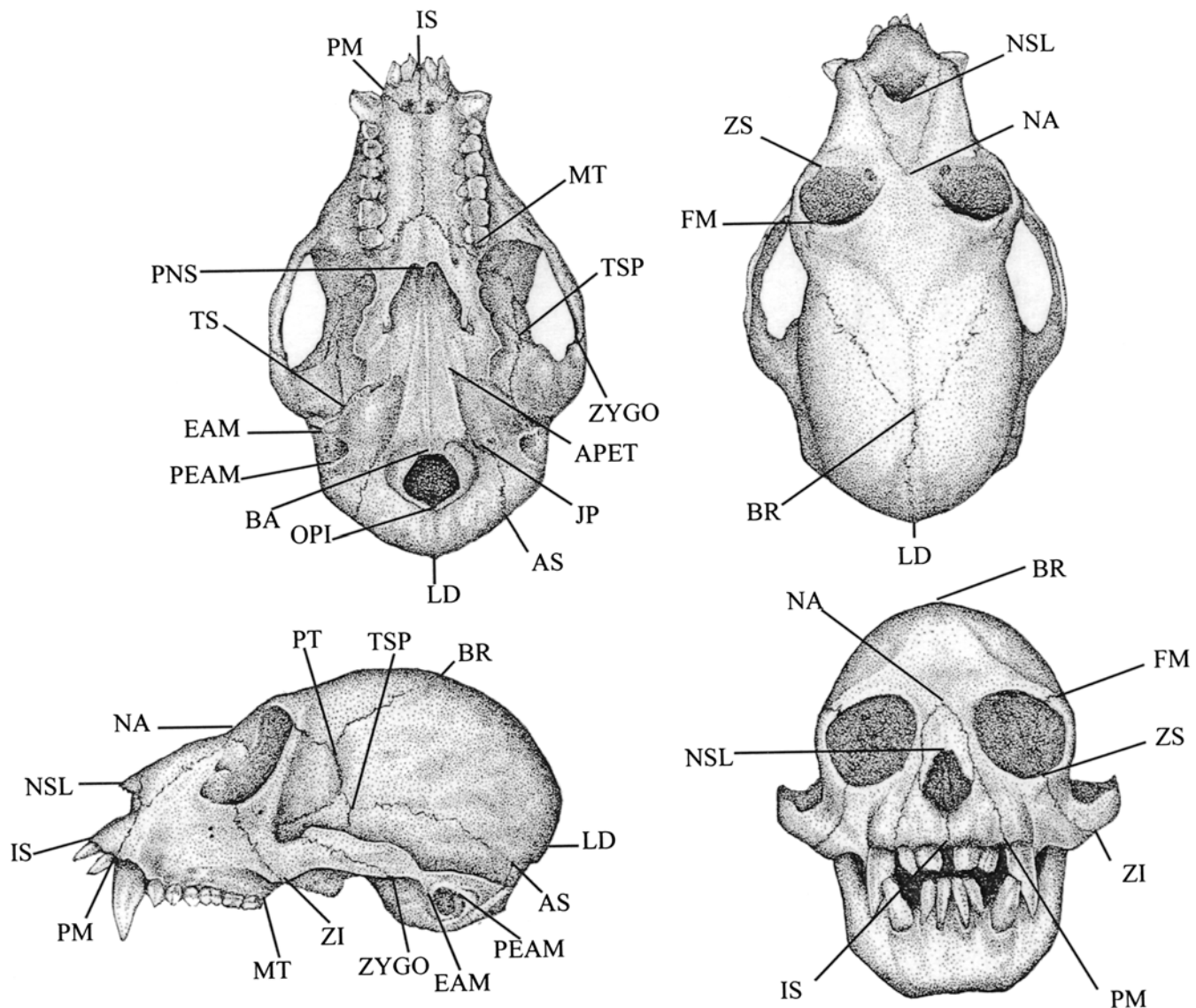
FIG. 1. Craniofacial landmarks recorded from New World monkey skulls using three-dimensional digitizer (see Marroig and Cheverud 2001 for landmarks and measurement details).

ancestral states for our continuous trait set using a maximum likelihood (ML) approach (Schluter et al. 1997) implemented in the program ANCML available from D. Schluter's home page (http://www.zoology.ubc.ca/~schluter/ancml.html). Although we use ML estimates, ancestral states reconstructed using maximum parsimony (MP) with the squared cost assumption (Maddison and Maddison 2003) result in virtually the same values. Tree topology and branch lengths were obtained from the same four-gene combined dataset used by Schneider et al. (2001). The Jukes-Cantor model was used to obtain the phylogenetic tree using the neighbor-joining method (Kumar et al. 2001). Our branch lengths (assumed to be roughly proportional to time) had a correlation of 0.993 with those reported by Schneider et al. (2001), with the largest difference being only 0.003 between the two datasets.

After the estimation of ancestral data, the direction of evolution (Δz) within each branch was obtained simply as the difference vector in the 39 averages of each taxon pair. It is important to keep in mind that ancestral nodes are reconstructions and not true ancestors relying on assumptions of character evolution and on the accuracy of the phylogeny (Omland 1999). While the tree we are using is highly supported statistically (Schneider et al. 2001), uncertainty about the root of the NWM tree is a cause of concern (see Schneider et al. 2001). We deal with this uncertainty using the two alternative hypotheses for the rooting of the NWM tree and redoing all analyzes to check the consistency of the results.

We compare the direction of evolution with both versions of LLER (g_{max} and p_{max}). While the genetic line of least evolutionary resistance (g_{max}) is unavailable for most taxa

TABLE 1. List of symbols used for the variables, how the variable was measured, and their biological meaning.

Symbol	Measure	Biological meaning
$\mathbf{W}$	Pooled within-groups variance/covariance matrix	The amount and pattern of variation and covariation within a group
$\mathbf{p_{max}}$	First principal component of the phenotypic $\mathbf{W}$	The linear combination of traits accounting for the largest portion of phenotypic variance within a group; the phenotypic line of least resistance to evolutionary change (LLER)
$\mathbf{g_{max}}$	First principal component of the genetic $\mathbf{W}$	The linear combination of traits accounting for the largest portion of genetic variance within a group; the genetic LLER
$\mathbf{\Delta_z}$	Vector of differences in the averages of any two groups	Direction of the evolution
m_{amount}	Sum of the squared differences in the averages of morphological traits of any two groups	The amount of morphological differentiation between two groups
m_{pace}	m_{amount} divided by the branch length	The pace of morphological change between two groups
d_{amount}	Sum of the squared differences in the averages of diet traits of any two groups	The amount of dietary differentiation between two groups
d_{pace}	d_{amount} divided by the branch length	The pace of dietary change between two groups
$\mathbf{L}$	Between-groups variance/covariance matrix obtained from the V/CV among-groups means	The amount and pattern of divergence among populations
total $\mathbf{p_{max}}$	First principal component of $\mathbf{L}$	The linear combination of traits accounting for the largest portion of phenotypic variance between groups
s_{dif}	Differences between any two groups average scores in the first principal component extracted from the between-groups ($\mathbf{L}$) V/CV matrix	The overall skull size difference between any two groups
b_{length}	Branch length in the NWM phylogenetic tree	Approximately the time between an ancestor and its immediate descendent
β	$\mathbf{W^{-1}\Delta z}$, or the inverse of $\mathbf{W}$ multiplied by the average differences between two groups	The pattern of selection responsible for species differences; a vector describing the reconstructed directional selection operating individually upon each trait independently from the other traits in the system
size	First principal component score of any group	Measures the absolute size of any genus
diet	Diet value for any genus based on the multidimensional scaling value obtained from the analyses of the diet similarity matrix	A combined measure of the diet of any genus; the MDS axis had negative values at one extreme for folivorous genera and conversely positive values for gum-insect feeding genera
β_{size}	Hypothetical pure isometric gradient selection vector	The pattern of selection upon size alone
Δz_h	Evolutionary response observed for the hypothetical β_{size} applied to each $\mathbf{W}$	The expected evolutionary response to selection on size alone

used here, we do have an estimate for it in the genus *Saguinus* (Cheverud 1996). This estimate of $\mathbf{g_{max}}$ was obtained as the first principal component (PC1) of the pooled within-groups additive genetic variance/covariance matrix of the two tamarin species studied by Cheverud (1996). We correlate this $\mathbf{g_{max}}$ with the $\mathbf{p_{max}}$ of each genus. If $\mathbf{p_{max}}$ is a reasonable proxy to $\mathbf{g_{max}}$ we expect that those correlations should be high. Throughout the paper whenever we refer to $\mathbf{g_{max}}$ we are referring to the PC1 obtained from the *Saguinus* additive genetic $\mathbf{W}$ matrix.

The direction of $\mathbf{p_{max}}$ was calculated from the $\mathbf{W}$ matrices as the PC1 for each taxon. This procedure is straightforward in the terminal branches of the tree (genus) but a bit less certain for the deepest nodes. The $\mathbf{W}$ covariance matrices were obtained for each node in the Platyrrhini tree, pooling all descendent genera from that node to estimate $\mathbf{W}$ and structuring the pooling according to the phylogeny. For example, the $\mathbf{W}$ matrix of node 30 (Fig. 2) involves the pooling of the $\mathbf{W}$ matrices of the genera *Callithrix* and *Cebuella*. Then, the $\mathbf{W}$ matrix of node 28 was obtained pooling the node 30 $\mathbf{W}$ matrix with the *Callimico* $\mathbf{W}$ matrix and so on through the whole phylogeny. Note that we are not taking into account the branch lengths in the estimation of ancestral $\mathbf{W}$ values, just the topology of the tree is used to direct the pooling.

This is justified by our previous finding of very similar $\mathbf{W}$ values among NWM and the independence of covariance matrix structural similarity relative to phylogenetic distance (Marroig and Cheverud 2001).

Finally, with both $\mathbf{\Delta z}$ and $\mathbf{p_{max}}$ (or $\mathbf{g_{max}}$) estimated, we obtain the angle (θ) formed between them as a measure of how closely morphological diversification follows the LLER. When evolutionary change occurs primarily along the LLER, θ will approach zero and, conversely, as $\mathbf{\Delta z}$ deviates more from $\mathbf{g_{max}}$, θ will increase. We used the cosine of the angle θ (vector correlation) to measure the relationship between $\mathbf{\Delta z}$ and $\mathbf{g_{max}}$ or $\mathbf{p_{max}}$ and therefore the smaller the angle the larger the correlation between vectors. Our strategy here was to focus on the evolutionary changes happening along each of the 30 branches on the tree and compare the direction of that change to the phenotypic and genetic lines of least resistance.

Lines of Least Evolutionary Resistance and the Amount and Pace of Morphological Change

Another question is whether the LLER influenced the amount and pace of morphological diversification. To answer this question, we first obtained a measure of the amount of morphological differentiation (m_{amount}) as the sum of squared

TABLE 2.   Analyses performed and corresponding symbols, how the analysis was performed, their biological meanings, and expectations.

Symbol	Measure	Biological meaning	Expectation
p_{max}-p_{max}	Vector correlation of the p_{max} of one group in relation to another group's p_{max}	How similar two groups are in their line of least evolutionary resistance (LLER)	Should be high for groups sharing the same orientation of the LLER and low for the reverse case
g_{max}-p_{max}	Vector correlation of the g_{max} of one group in relation to another group's p_{max}	How similar two groups are in their phenotypic and genetic LLER	Same as above
Δz-g_{max}	Vector correlation between Δz and g_{max}	How closely the direction of evolution follows the genetic LLER	Should be high if the genetic LLER influences the evolutionary path
Δz-p_{max}	Vector correlation between Δz and p_{max}	How closely the direction of evolution follows the phenotypic LLER	Should be high if the phenotypic LLER influences the evolutionary path
Branch length $\times$ amount and pace measures	Pearson product moment correlation	The association between time (branch length) and the amount and pace of evolution	Should be positive if longer time allows for more differentiation to accumulate; no a priori association expected in terms of the pace through time
Branch length $\times$ Δz-p_{max} and Δz-g_{max}	Pearson product moment correlation	The temporary nature of the effect of the LLER on evolution	A negative association is expected if the bias in the evolutionary trajectory imposed by the LLER is temporary
Δz-p_{max} and Δz-g_{max} $\times$ amount and pace measures	Pearson product moment correlation	Whether the amount and pace of evolutionary change is associated with how close to the LLER the direction of evolution was	Positive associations are expected, because when the evolutionary change occurs away from the LLER, genetic variance along those other dimensions are relatively low, reducing the amount and pace of evolutionary response
S_{dif} $\times$ branch length, amount and pace measures and Δz-p_{max} and Δz-g_{max}	Pearson product moment correlation	The association between the absolute skull size (or body size) differences with time, pace, and amount and how closely to the LLER the direction of evolution was	Positive associations are expected when large niche-related differences are related to size differences, if time elapsed allow for larger size differences to accumulate, and when overall mophological differences are mostly size differences
β $\times$ p_{max}	Pearson product moment correlation	Tests the hypothesis that directional selection is similar to LLER	Should be high if selection is aligned with the LLER
β $\times$ Δz	Pearson product moment correlation	Tests an alternative hypothesis to LLER, that the direction of evolution reflects the orientation of the directional selection	Should be high if evolutionary response is aligned with selection
Δz $\times$ Δz_h	Vector correlation between Δz and Δz_h	Tests the hypothesis that selection on size alone would produce evolutionary responses close to those observed	Should be high if selection upon size alone would result in responses similar to those observed

differences of the averages for the 39 traits for each of the 30 internodes. A measure of the pace of morphological differentiation (m_{pace}) was obtained dividing the m_{amount} by the length of the corresponding branch on a genetic distance scale. We then compare m_{amount} and m_{pace} with the Δz-p_{max} and Δz-g_{max} using Pearson product moment correlation. If selection favors divergence in a direction markedly different from that of the LLER, the expectation is that the evolutionary amount and pace should be relatively small and slow respectively (Schluter 1996). The reason is straightforward: directions other than the g_{max} (or p_{max}) have less genetic variance, reducing the amount and rate of the evolutionary response expected along those other lines given the same intensity of directional selection. Therefore, a negative correlation of the amount and pace of morphological differen-

tiation and θ (or a positive correlation if the cosine of the angle Δz-p_{max} is used) is expected.

Allometric Size and Absolute Size

It is important to keep in mind that size has two meanings here. Absolute size refers to the overall body size of an animal (or an estimator of it like the PC1 score), whereas p_{max} or allometric size refers to the allometry of one variable with respect to the size variation in a population of organisms of different absolute sizes, being therefore a measure of the relative contribution of each variable to absolute size. In other words, p_{max} is a measure of variation, whereas absolute size is a measure of the average skull (or body) size. Absolute skull size was obtained as the score on the PC1 extracted from the between-populations V/CV matrix **L** (**L** is the V/
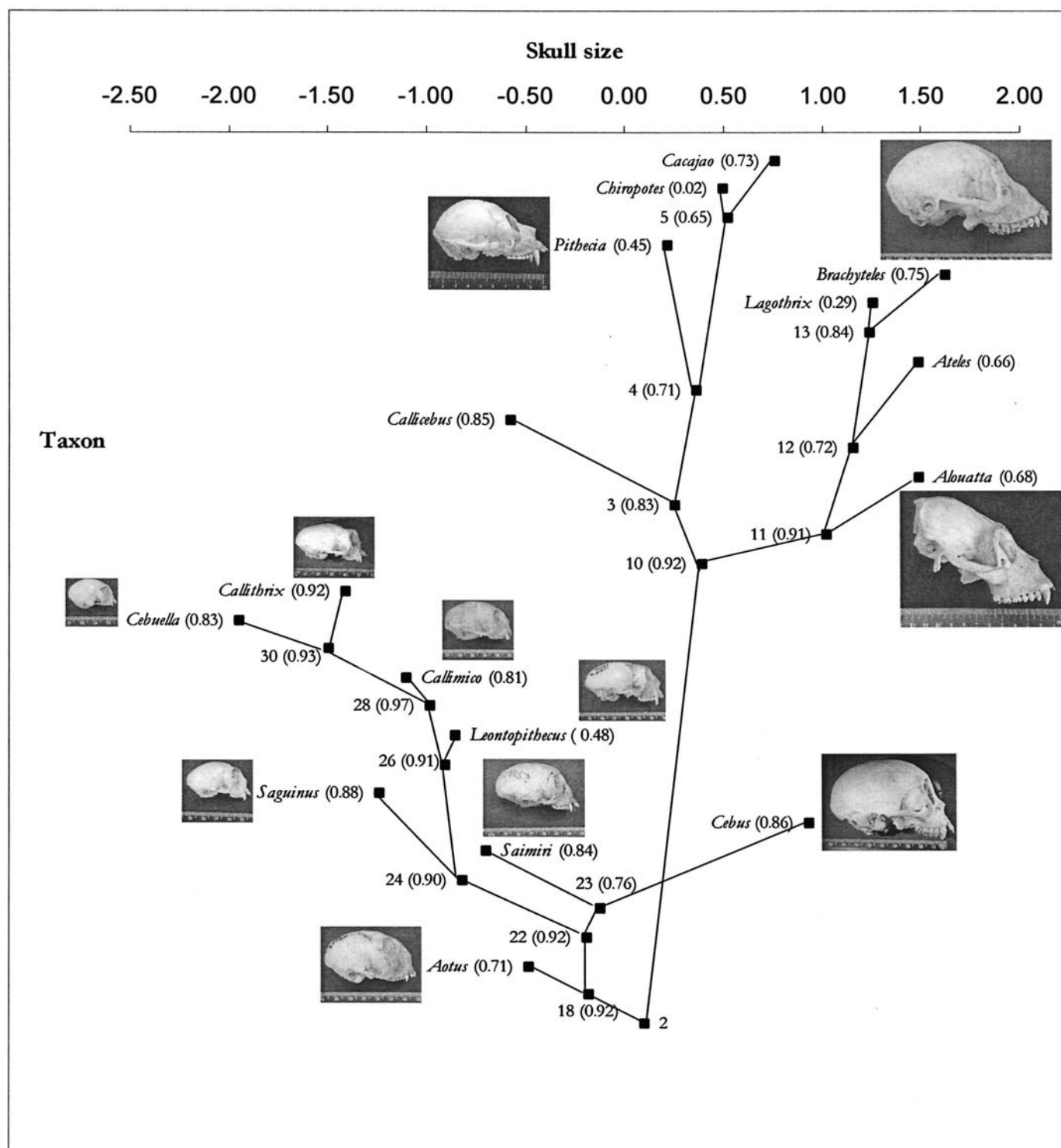
FIG. 2. Skull size estimated from a principal component analysis on the 39 trait averages of all living and ancestor estimates (numbered nodes) of New World monkeys. The phylogenetic tree, with arbitrary branches lengths, is superimposed on the skull PC1 scores. Skull pictures are proportional to skull sizes. The Δz-p_{max} values are shown within parenthesis after the name or number of each genus or node corresponding to a branch end.

CV constructed from the 16 living genera and 15 ancestral nodes population means). This between-taxon PC1 accounts for 92.8% of the total variation among groups. For the 16 living genera, the correlation between estimated skull size and their body weights (Fleagle 1999) is 0.987 ($P < 0.0001$), indicating that the PC1 scores are a good proxy for overall body size. Absolute skull size differences (s_{dif}) were obtained from the squared differences in the PC1 (extracted from **L**) scores of each pair of taxa. This measure (s_{dif}) is used here because is quite possible that large size differences are related to niche differentiation and time elapsed as well as with the LLER (Table 2). Allometric size ($\mathbf{p_{max}}$) was compared in two ways. First, we estimated the pairwise vector correlations among the PC1 values of each living genus. This is a measure of similarity of the two vectors and an explicit measure among NWM genera of the existence and strength of the LLER and of their persistence through time when coupled with phylogenetic information (Maynard Smith et al. 1985; Arnold 1992; Schluter 1996). Second, we obtained PC1s for the **W** matrices of each node in the tree ($\mathbf{p_{max}}$) and focus on the similarity of those PC1s structuring our comparisons at each of the 30 internodes on the tree in the same way we did for comparisons between $\mathbf{\Delta z}$ and $\mathbf{p_{max}}$ or $\mathbf{g_{max}}$ (see above).

Phylogeny and Diet

Diet similarity and phylogenetic distances were previously reported by us (Marroig and Cheverud 2001). In addition, we also estimate the diet of ancestral states using the same procedure (ML) described above for the quantitative traits. With the averages estimated for the five dietary variables (fruits, insects, gum, seeds, and leaves) we also obtained measures of the amount and pace of evolutionary change in diet for each branch in the tree. The amount of dietary change (d_{amount}) was obtained as the sum of the squared differences of the averages for the diet variables for each of the 30 internodes. Likewise, the pace of dietary change (d_{pace}) was obtained by dividing d_{amount} by the corresponding branch lengths. Finally, from the dietary similarity matrix we obtained a combined measure comparable to the absolute size measure (PC1). This was done by performing a multidimensional scaling analysis (MDS) on the dietary similarity matrix and using only one axis to represent this ecological variable. This allows us to test whether size and diet evolution are significantly associated.

Lines of Least Evolutionary Resistance Association with Size and Diet

Correlation between diet (d_{pace} and d_{amount}) morphological (m_{pace} and m_{amount}) and absolute skull size differences (s_{dif}) as well as their associations with $\mathbf{\Delta z}$-$\mathbf{g_{max}}$ and $\mathbf{\Delta z}$-$\mathbf{p_{max}}$ were obtained. Because the changes occurring within each branch are independent from the other branches, a standard Pearson correlation coefficient was used. Many of these variables were nonnormal and therefore some transformations were applied before analyses. Fisher's transformation was used to normalize the $\mathbf{\Delta z}$-$\mathbf{g_{max}}$ and $\mathbf{\Delta z}$-$\mathbf{p_{max}}$ correlation values, and a square-root transformation was used to normalize the diet pace and amount variables as well as branch lengths. Morphological pace and m_{amount} were transformed by obtaining

their natural logarithms. Skull size difference (s_{dif}) was normalized by multiplying the original values by a constant (10,000) and then obtaining its natural logarithm. To correct for multiple testing, we use the approach outlined in Cheverud (2001) to estimate the number of effective independent comparisons and then applied the Bonferroni correction to adjust the alpha level.

Diet can be conceived as being organized into broad adaptive zones in NWM (Figs. 2, 3). The invasion of new diet-based adaptive zones occurred four times during the Platyrrhine diversification. All NWM eat fruits, allowing for variation in the proportion consumed and of the other items used to supplement their diets. Each of the four other diet categories (seeds, insects, gum, and leaves) define four distinct clades within Platyrrhini. If the invasion of new dietary adaptive zones was one key factor unleashing adaptive radiation along LLER in Platyrrhini, we expect that the largest transitions in absolute size as well as the largest $\mathbf{\Delta z}$-$\mathbf{p_{max}}$ and $\mathbf{\Delta z}$-$\mathbf{g_{max}}$ correlations to occur in those branches associated with the invasion of new diet zones. Invasion of new dietary zones occurred at the following internodes (see Fig. 2): 10–3 (the seed zone), 10–11(leaf zone), 22–24 (gum zone), 2–18 (insect zone), and 2–10 (leaf-seed). We used one-tailed t-tests with unequal variances to detect whether the values at these internodes were significantly different from those of the others.

Retrospective Selection, g_{max}, and the Direction of Evolution

The appraisal of the similarity between $\mathbf{\Delta z}$ and $\mathbf{g_{max}}$ as evidence for genetic constraints rests on the assumption that the direction of divergent natural selection is random with respect to the direction of $\mathbf{g_{max}}$ (Schluter 2002). An alternative hypothesis is that selection, rather than genetic constraints, is responsible for the bias in the direction of divergence (Schluter 2002). In such a scenario, the direction of evolution ($\mathbf{\Delta z}$) is closely aligned with $\mathbf{g_{max}}$ because selection corresponds to $\mathbf{g_{max}}$. The evolutionary response of a set of quantitative traits is described by the equation $\mathbf{\Delta z} = \mathbf{G\beta}$, where $\mathbf{\Delta z}$ is the vector of differences in means between generations, $\mathbf{\beta}$ is the selection gradient vector, and $\mathbf{G}$ is the additive genetic V/CV matrix (Lande 1979). Rearranging the evolutionary response equation, the pattern of selection responsible for species differences can be reconstructed from observed mean differences using the following relationship:

$$\mathbf{\beta} = \mathbf{G}^{-1}(\bar{z}_i - \bar{z}_j), \qquad (1)$$

where $\mathbf{\beta}$ is the cumulative differential selection gradient summed over generations, $\mathbf{G}^{-1}$ is the inverse of the additive genetic V/CV matrix, and $(\bar{z}_i - \bar{z}_j)$ is the difference in means between species i and j or $\mathbf{\Delta z}$ for simplicity here (Lande 1979; Lofsvold 1988; Cheverud 1996).

The following relationship was used to obtain the selection gradients:

$$\mathbf{\beta} = \mathbf{W}^{-1}\mathbf{\Delta z}, \qquad (2)$$

where $\mathbf{\Delta z}$ is the difference vector between two nodes (or between a living genus and its ancestor), and $\mathbf{W}^{-1}$ is inverse of the phenotypic pooled within-group covariance matrix. We compare the selection gradients $\mathbf{\beta}$ with the $\mathbf{\Delta z}$ and $\mathbf{p_{max}}$ using
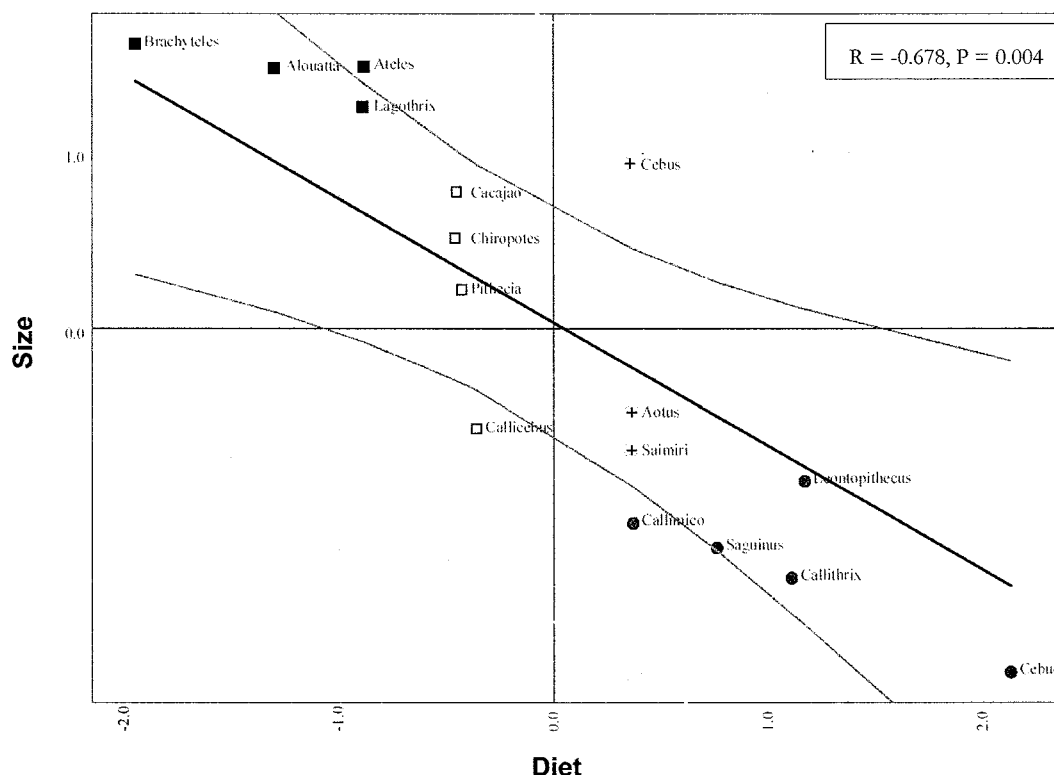
FIG. 3. Plot of the absolute skull size against diet (the multidimensional scaling value obtained from the diet similarity 16×16 matrix). The regression line and 95% confidence limits were obtained from the method described in Garland and Ives (2000) and implemented in package PDAP in Mesquite. Black squares, leaves-fruits; open squares, seed-fruits; gray squares with cross inside, insect-fruits; black circles, gum-insect-fruits.

vector correlation. When selection is along both vectors, we expect a high correlation of the gradients with the difference vector Δz and with the direction of maximum phenotypic variance.

RESULTS

The standardized PC1 ($\mathbf{p_{max}}$) extracted from each of the 16 pooled generic within-species covariance matrices is presented in Table A1 (available online only at http://dx.doi.org/10.1554/04-333.1.s1). Table A1 also presents the eigenvalues and the percent of the total variance explained by each component. The percent of within-taxon variance explained by the PC1 ranges from 20% to 40%. Additionally, Table A1 (available online) also presents the pooled tamarin $\mathbf{g_{max}}$ and its correlation with the allometric vector ($\mathbf{p_{max}}$) for each genus. The smallest correlation observed for $\mathbf{g_{max}} \times \mathbf{p_{max}}$ among the living NWM genera was 0.74 in *Cebuella* and the average was 0.852 (SD = 0.051). The full table with the vector correlations between PC1s comparing each pair of genera is presented in Table A2 (available online only at http://dx.doi.org/10.1554/04-333.1.s2). Raw generic allometric-size vector correlations average 0.857 (SD = 0.068) and, after adjusting for sampling error (Marroig and Cheverud 2001), average 0.909 (SD = 0.060). Comparisons of $\mathbf{p_{max}}$ values along individual branches of the tree (Table 3) reveal an even higher level of allometric pattern conservation (vector correlation average 0.97, SD = 0.05). Most of the 30 ancestor-descendent PC1 correlations are above 0.94, with

only a few below that level (*Leontopithecus*, node 26 = 0.92; *Callimico*, node 28 = 0.89; *Cebuella*, node 30 = 0.83; *Brachyteles*, node 13 = 0.80).

Figure 2 shows the NWM tree with numbered nodes and with arbitrary branch lengths. The values of Δz-$\mathbf{p_{max}}$ are presented for each of the 30 internodes along the tree. Table 4 presents the correlation and associated significance among Δz-$\mathbf{p_{max}}$, Δz-$\mathbf{g_{max}}$, branch lengths, absolute size differences, and amount and pace of change in morphology and diet. The significance test was one-tailed because the alternative hypothesis of interest is whether there is a positive relationship among all variables. The effective number of independent correlations was estimated by the number of significant eigenvalues, which may be extracted from the 28 observed correlations. We found that four eigenvalues can be extracted and therefore our experimentwise significance threshold was $P = 0.013$ (0.05/4). Absolute size differences (s_{dif}) show positive, significant correlations with b_{length}, m_{amount}, m_{pace}, Δz-$\mathbf{p_{max}}$, and Δz-$\mathbf{g_{max}}$. The branch lengths are positively and significantly correlated with morphological and dietary amount of change, indicating that the longer the time since separation of two taxa, the larger the differences in morphology and diet. The amount of morphological differentiation is positively and significantly associated with the m_{pace} and d_{amount}. However, the association of the amount of morphological change with Δz-$\mathbf{g_{max}}$ and Δz-$\mathbf{p_{max}}$ is close to zero and is not significant. Dietary amount and pace of change are positively associated with each other, but there is no

TABLE 3. For each pair of ancestor-descendent the vector correlations between p_{max} values, directional selection gradients β and p_{max}, and divergence vector Δz and β are shown. The vector correlations between Δz and the genetic (g_{max}) and phenotypic (p_{max}) axes of maximum variance are also shown. Associated branches lengths are presented. The last column shows the vector correlation between observed Δz values and the ones obtained using a hypothetical isometric size selection vector. Genus-ancestor numbers refer to the nodes in Figure 2.

Genus-ancestor	p_{max}-p_{max}	$\beta \times p_{max}$	$\beta \times \Delta_z$	Δz-g_{max}	Δz-p_{max}	b_{length}	$\Delta z \times \Delta z_h$
23–22	0.99	0.05	0.25	0.82	0.76	0.0033	0.77
30–28	1.00	0.10	0.21	0.91	0.93	0.0122	0.96
28–26	1.00	0.14	0.27	0.93	0.97	0.0016	0.97
26–24	0.99	0.15	0.35	0.90	0.91	0.0019	0.93
24–22	0.95	0.09	0.25	0.90	0.90	0.0094	0.94
2–10	0.99	0.10	0.28	0.88	0.92	0.0052	0.94
22–18	1.00	0.05	0.29	0.81	0.84	0.0003	0.90
18–2	0.98	0.10	0.28	0.88	0.92	0.0050	0.94
11–10	1.00	0.08	0.26	0.84	0.91	0.0079	0.92
11–12	0.96	0.04	0.33	0.78	0.72	0.0024	0.73
13–12	0.98	0.04	0.29	0.80	0.84	0.0030	0.86
10–3	0.98	0.04	0.29	0.73	0.83	0.0057	0.85
5–4	0.99	0.03	0.32	0.67	0.65	0.0066	0.66
4–3	1.00	0.02	0.39	0.79	0.71	0.0087	0.72
Pithecia-4	0.99	0.01	0.31	0.41	0.45	0.0124	0.45
Callicebus-3	0.98	0.09	0.32	0.86	0.85	0.0226	0.88
Ateles-12	0.97	0.04	0.36	0.65	0.66	0.0125	0.66
Alouatta-11	1.00	0.03	0.39	0.42	0.68	0.0200	0.68
Aotus-18	0.94	0.02	0.29	0.74	0.71	0.0227	0.72
Saguinus-24	1.00	0.10	0.31	0.88	0.88	0.0215	0.90
Leontopithecus-26	0.92	0.02	0.48	0.41	0.48	0.0165	0.45
Callimico-28	0.89	0.03	0.26	0.70	0.81	0.0149	0.75
Callithrix-30	1.00	0.08	0.39	0.88	0.83	0.0047	0.86
Cebuella-30	0.83	0.11	0.24	0.94	0.92	0.0077	0.96
Cebus-23	1.00	0.03	0.11	0.89	0.86	0.0256	0.90
Saimiri-23	0.95	0.02	0.20	0.77	0.84	0.0307	0.88
Brachyteles-13	0.80	0.02	0.22	0.67	0.75	0.0132	0.78
Lagothrix-13	0.99	0.01	0.22	0.35	0.29	0.0129	0.22
Cacajao-5	0.98	0.03	0.28	0.78	0.73	0.0093	0.78
Chiropotes-5	0.99	0.00	0.38	0.12	0.02	0.0096	0.06

association between them with Δz-g_{max} and Δz-p_{max}. Finally, Δz-g_{max} and Δz-p_{max} are strongly associated. The association analyses based on the IC show the same overall pattern (Table 5) as the analyses based on the internodes approach (Table 4), but with some interesting differences. Noteworthy is the positive and significant association of m_{amount} and m_{pace} with Δz-g_{max} and Δz-p_{max}. Diet amount and pace of change, while not significantly correlated using our conservative correction for multiple tests, present positive, moderate associations with both the amount and pace of morphological evolution. The MDS axis accounts for 93.6% of all variation in the diet similarity matrix and had negative values at one end for leaf-eaters and positive values at the other extreme for the gum-eaters (Fig. 3). Absolute size is significantly correlated with diet ($R = -0.678$, $P = 0.004$) using the independent contrasts (Fig. 3).

To test the predictions that the largest transitions in absolute size as well as the largest Δz-p_{max} correlations occur in those branches associated with the invasion of new diet zones we applied a *t*-test comparing those values between two groups: new invasion ($n = 5$), corresponding to the above cited branches and stable ($n = 25$), corresponding to all other branches. Because the two groups have very unequal sample sizes an unequal variance *t*-test was applied. All averages were higher in the new invasion group, with significant differences observed for Δz-p_{max} ($t = 3.659$, df = 17.7, $P =$

TABLE 4. Correlation between absolute skull size differences (s_{dif}), branch length (b_{length}), morphological amount and pace of evolutionary change (m_{amount} and m_{pace}), diet amount and pace of change (d_{amount} and d_{pace}), and the vector correlation between divergence vector (Δz) genetic (g_{max}) and phenotypic (p_{max}) axes of maximum variance (Δz-g_{max} and Δz-p_{max}) are shown below the diagonal. Associated probabilities are above the diagonal. Bonferroni-corrected significant values are in bold and marginally significant values are in italic.

	s_{dif}	b_{length}	m_{amount}	m_{pace}	d_{amount}	d_{pace}	Δz-g_{max}	Δz-p_{max}
s_{dif}	1	**0.002**	**0.000**	**0.000**	*0.019*	0.064	*0.013*	**0.011**
b_{length}	**0.530**	1	**0.000**	*0.050*	**0.003**	0.229	0.182	0.154
m_{amount}	**0.850**	**0.790**	1	**0.000**	**0.001**	*0.027*	0.702	0.665
m_{pace}	**0.840**	*0.360*	**0.830**	1	*0.031*	0.069	*0.036*	*0.022*
d_{amount}	*0.420*	**0.520**	**0.580**	*0.390*	1	**0.000**	0.876	0.971
d_{pace}	0.340	0.230	*0.400*	0.340	**0.920**	1	0.554	0.546
Δz-g_{max}	*0.450*	−0.250	0.070	*0.390*	−0.030	0.110	1	**0.000**
Δz-p_{max}	**0.460**	−0.270	0.080	*0.420*	−0.010	0.110	**0.920**	1

TABLE 5. Correlation obtained from the independent contrasts between s_{dif}, b_{length}, m_{amount}, m_{pace}, d_{amount}, d_{pace}), Δz-g_{max} and Δz-p_{max} are shown below the diagonal. Associated probabilities are above the diagonal. Bonferroni-corrected significant values are in bold and marginally significant values are in italic.

	s_{dif}	b_{length}	m_{amount}	m_{pace}	d_{amount}	d_{pace}	Δz-g_{max}	Δz-p_{max}
s_{dif}	1	0.066	**0.000**	**0.000**	0.062	0.097	**0.000**	**0.000**
b_{length}	0.393	1	**0.002**	*0.036*	0.256	0.455	0.371	0.193
m_{amount}	**0.834**	**0.666**	1	0.966	*0.016*	*0.041*	**0.012**	**0.002**
m_{pace}	**0.866**	*0.462*	0.966	1	*0.013*	*0.019*	**0.002**	**0.000**
d_{amount}	0.401	0.177	*0.539*	0.556	1	**0.000**	0.163	0.068
d_{pace}	0.343	−0.031	*0.447*	0.522	**0.964**	1	0.125	0.073
Δz-g_{max}	**0.765**	0.089	**0.563**	**0.676**	0.262	0.306	1	**0.000**
Δz-p_{max}	**0.889**	0.232	**0.682**	**0.756**	0.389	0.381	**0.936**	1

0.001), Δz-g_{max} ($t = 1.967$, df = 12.0, $P = 0.036$), and s_{dif} ($t = 2.093$, df = 10.8, $P = 0.030$), while m_{amount} was deemed not significant at the 5% level and m_{pace} was marginally significant ($t = 1.962$, df = 5.6, $P = 0.050$).

The comparisons of $\boldsymbol{\beta}$ with $\mathbf{p_{max}}$ (Table 3) reveal virtually no relationship between the selection gradient and the maximum variance axis ($\bar{X} = 0.056$, SD = 0.041). The same pattern holds for the comparison of $\boldsymbol{\beta}$ with $\Delta \mathbf{z}$ (Table 3, Fig. 4) but here the overall average ($\bar{X} = 0.295$, SD = 0.072) is close to the upper limit (0.41) of the 99% confidence interval expected for the correlation of two random 39-element vectors.

DISCUSSION

Allometry, Line of Least Resistance, and Evolutionary Divergence

NWM genera share the same basic allometric patterns ($\mathbf{p_{max}}$) of variation in skull morphology. This allometric vector represents the line of least evolutionary resistance. Given the considerable differences in absolute size among NWM and their deep history (at least 30 million years of evolutionary diversification), there is surprising conservation of shape variation associated with size. Allometric size accounts for 20–40% of all variation within each taxon. Differences in absolute skull size, as measured by the between genera PC1, accounts for 92.8% of the total variation among genera and is very similar (**total $\mathbf{p_{max}}$** in Table A1, available online) to the within genus PC1s (vector correlation $\bar{X} = 0.86$, SD = 0.066). This simple result suggests that morphological divergence between genera follows the within-population allometric line. The conservation of allometric patterns is even more striking when we consider that it is not only a phenotypic pattern but also reflects the genetic architecture underlying it. This is reflected in the correlation between $\mathbf{g_{max}}$ and $\mathbf{p_{max}}$ ($\bar{X} = 0.852$, SD = 0.051) uncorrected in this case for sampling error, but still fairly high. Given the striking similarity in $\mathbf{g_{max}}$ and $\mathbf{p_{max}}$ found here, we consider both interchangeable for the purpose of the discussion below (Table 3). A genetic LLER therefore appears to exist in NWM and to have persisted for at least 30 million years. But did that LLER influence the paths of evolutionary diversification for NWM crania?

An inspection of the $\Delta \mathbf{z}$-$\mathbf{p_{max}}$ in Figure 2 (see also Table 3) reveals that most of the diversification in NWM follows the LLER defined by size, with the $\Delta \mathbf{z}$-$\mathbf{p_{max}}$ correlation usu-

ally in the range of 0.85 to 0.97. Moreover, the high correlation between absolute size differences and m_{amount} also shows that most of the morphological diversification in NWM was related to size diversification (a result also consistent with the high correlation between **total $\mathbf{p_{max}}$** and the $\mathbf{p_{max}}$ values, Table A1, available online). While in NWM these two measures of morphological differentiation are very highly correlated, there is no a priori reason why they should be. Keep in mind that m_{amount} is a measure of how much two groups differ in overall morphology (not only size), whereas s_{dif} is a measure of the absolute size differences between two groups. This result is robust to alternative topologies of the phylogenetic tree (results not shown), where the root is placed in the Atelinae or in the Pithecinae clades before reconstruction of the ancestor states, supporting that evolution followed $\mathbf{p_{max}}$ or $\mathbf{g_{max}}$ (Table 3) during the NWM radiation.

However, there are also many instances where the direction
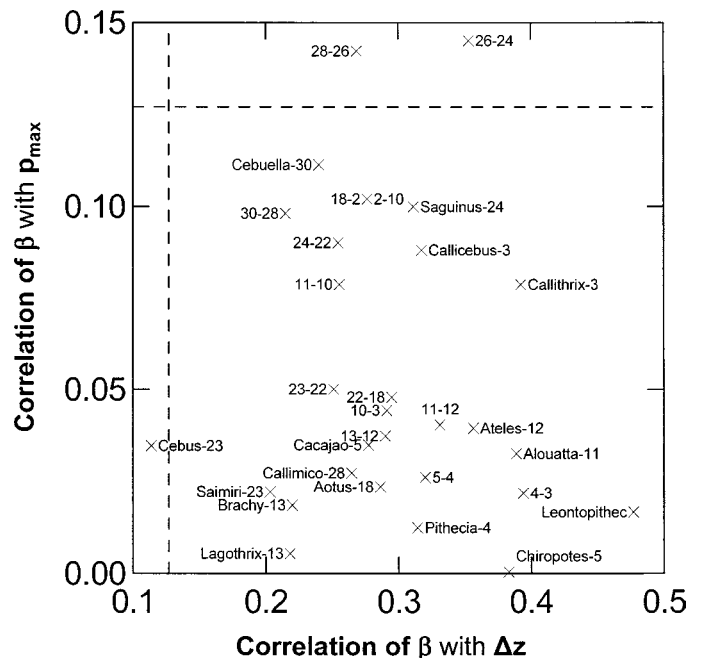
FIG. 4. Plot of the vector correlations between the reconstructed selection gradients ($\boldsymbol{\beta}$) and the evolutionary responses ($\Delta \mathbf{z}$) on the x-axis and the vector correlations of $\boldsymbol{\beta}$ with $\mathbf{p_{max}}$ in the y-axis. The dashed lines show the null expectation of 0.127 for a vector correlation of 39 elements. Numbers within the graph refer to the nodes in Figure 2.

FIG. 5. Plot of branch lengths (transformed to their squares roots) and Δz-p_{max} vector correlation (Fisher transformed). The dashed line shows the null expectation of 0.127 for a vector correlation of 39 elements. Numbers within the graph refer to the nodes in Figure 2.
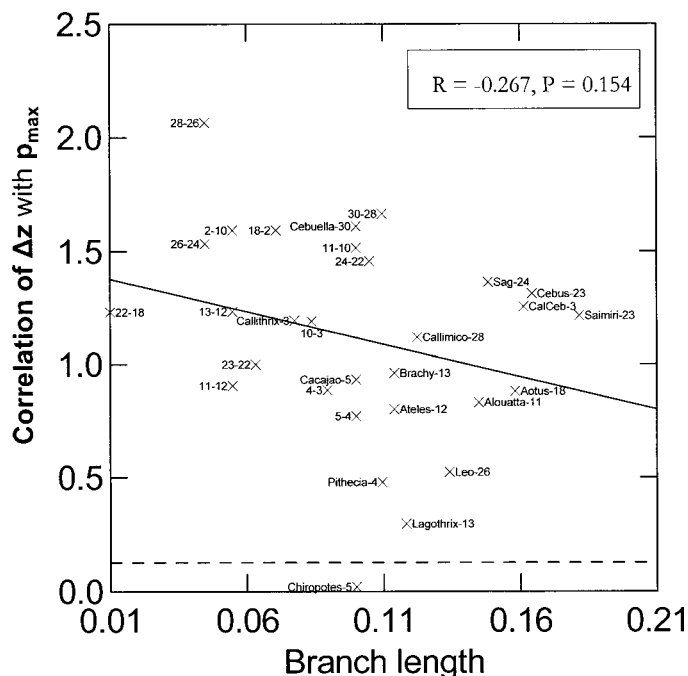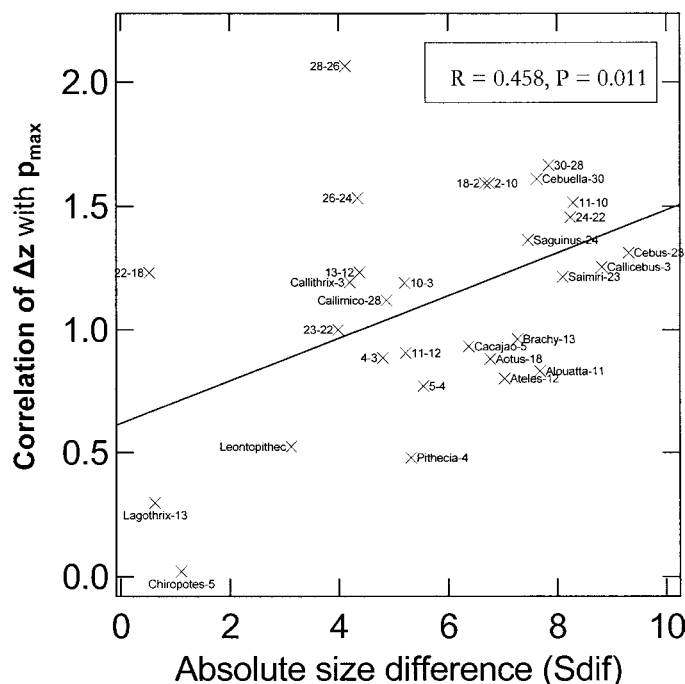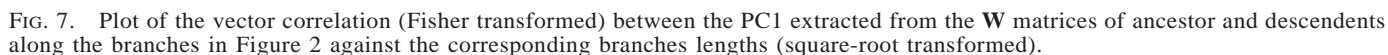

FIG. 6. Plot of the Δz-p_{max} vector correlation (Fisher transformed) against the absolute size differences. Numbers within the graph refer to the nodes in Figure 2.

of evolutionary change is remarkably distinct from the size dimension. Examples are *Leontopithecus*, *Lagothrix*, *Chiropotes*, and *Pithecia*, all showing values of Δz-p_{max} close to or below that of random expectation (Figs. 2, 5). These four cases are exactly those where the size differences between ancestors and descendents are the smallest (Fig. 6) observed in the tree ($t = 3.217$, df = 3.8, $P = 0.034$). Therefore, whenever evolution proceeded in a direction remarkably different from the LLER, the absolute size differences were also comparatively small. It is also interesting to note that those four cases with lower Δz-p_{max} values also had a slower pace of morphological change (m_{pace}, $t = 4.019$, df = 7.6, $P = 0.002$) compared to the remaining cases, but while the amount of morphological change on average is smaller in those four genera (m_{amount}, $t = 1.672$, df = 18.7, $P = 0.055$) this last result is not significant. The difference in these two results is basically due to node 22, which has a very small amount of morphological change relative to its last common ancestor (node 18) but has a very high pace of morphological change due to its very short branch length. Excluding internode 22–18 from the comparison, the *t*-test results are: m_{amount}, $t = 2.238$, df = 15.9, $P = 0.020$ and m_{pace}, $t = 4.156$, df = 7.7, $P = 0.002$. These results suggest that when evolution does not occur along the LLER, the amount and pace of morphological change are small and slow respectively, which is also apparent in the association analysis results presented in Tables 4 and 5. This is in agreement with the expectation advanced by Schluter (1996) that evolution should be slower when selection favors divergence in a direction markedly different from that of g_{max}. Therefore, taking these results together, there is support for the view that the LLER influ-

enced the path, rate, and amount of morphological evolution in NWM at a macroevolutionary scale.

We now address two final and related questions about the LLER: How much diversification is allowed along such lines and for how long do those lines persist? Conceivably, natural selection can change the patterns of morphological integration either by actively building new adaptive trait ensembles (Berg 1960; Baker and Wilkinson 2003; Bégin and Roff 2003) or indirectly while changing the averages of evolving populations and consequently affecting correlation among traits (Marroig and Cheverud 2001; see also Jones et al. 2004). By altering morphological integration patterns, selection should also change the lines of least resistance. Therefore, in an adaptive radiation it is reasonable to expect that at some point the lines of least resistance will diverge in orientation. Schluter (1996) predicted that the bias in evolutionary direction should be temporary and diminish with time. Our results here are mixed. First, there is indeed a trend of longer branches being associated with lower Δz-p_{max} correlations (Fig. 5, Table 4), but those correlations are not significant. Also, there is a negative correlation of the p_{max}-p_{max} vector correlations (Table 3) and their associated branch lengths (Fig. 7), indicating that p_{max} itself is diverging with time. One possible explanation for such a pattern is that any correlation between these vectors (Δz-p_{max} or p_{max}-p_{max}) at the tips of the tree is compounded at deeper nodes given our strategy of reconstructing ancestral states. However, a comparison of deeper nodes against tips in the tree after excluding the outliers discussed above (see also Figs. 5, 7) show no significant difference between the two groups with respect to the similarity in p_{max} orientation, suggesting that compounded error is not responsible for this pattern. Moreover,

FIG. 7. Plot of the vector correlation (Fisher transformed) between the PC1 extracted from the **W** matrices of ancestor and descendents along the branches in Figure 2 against the corresponding branches lengths (square-root transformed).

using the IC approach to compute the correlation between Δz-p_{max} (Table 5) or p_{max}-p_{max} ($R = -0.139$, $P = 0.605$) with branch length reveals no association among them. Conversely, longer branches are concentrated at the tips of the NWM tree ($t = -5.28$, df $= 27$, $P < 0.0001$), which might well explain why deeper nodes present higher correlations (less time to diverge). Second, while this trend occurs within branches, on a macroevolutionary scale the g_{max} and p_{max} conservatism discussed above suggests that allometric size acts as a LLER during the whole period of the NWM radiation, with no trend to diminish with time's arrow. This conclusion is also reinforced by the low and nonsignificant matrix correlation followed by a Mantel test ($R = 0.013$, $P = 0.552$) observed between phylogenetic distances and similarity in p_{max} (Table A2, available online). The amount of cranial morphological diversification occurring in NWM along the LLER might be quantified as the relative difference in skull size between the extremes of variation observed in Figure 2. *Brachyteles*' skull is 3.57 times bigger than the skull of *Cebuella*, which corresponds to an 81-fold difference in body mass (Fig. 2). Another measure of the amount of morphological diversification occurring in NWM along the LLER is the between groups PC1 eigenvalue, which inform us that 92.8% of the total variation is due to size changes (given the similarity between **total p_{max}** and the p_{max} values). Therefore, in NWM there is weak support for the prediction that the bias in the direction of evolution imposed by the LLER should be temporary and diminish with time. Our results indicate that not only the LLER endured on a macroevolutionary scale but also allowed for a large amount of diversification without changing its orientation.

Adaptive Radiation, Size Evolution, and Diet

Adaptive radiation is the evolution of ecological and phenotypic diversity within a rapidly multiplying lineage (Schluter 2002). Four features might be used to detect an adaptive radiation according to Schluter (2002): common ancestry, phenotype-environment correlation, trait utility (fitness advantage), and rapid speciation. All NWM share a common ancestor and we have indirect evidence for cranial trait utility (Marroig and Cheverud 2004). The indirect evidence came from the analyses of morphological evolution in NWM showing that natural selection dominated their diversification, particularly at the levels of the origins of families, subfamilies, and genera, and especially upon size (Marroig and Cheverud 2004). Rapid speciation occurred when the three NWM families emerged nearly simultaneously (Schneider et al. 2001) at the Oligocene–Miocene boundary (26 million years ago) giving rise to three of the four major diet adaptive types in a burst of diversification (Atelidae, leaves; Pitheciidae, seeds; Cebidae, insects). The correlation between form and function is not totally established, at least not quantitatively, because association of skull morphology and environmental factors (like diet) are still sparse for NWM (Rosenberger et al. 1996). However, the association of diet with skull morphology is clear in our results (Fig. 3, see also Marroig and Cheverud 2001). Considering these four features, the evolution of NWM might be considered an adaptive radiation resulting today in more than 110 living species (Rylands et al. 2000) occupying many adaptive zones related to diet, locomotion, systems of mating, and habitats.

We suggested before that the adaptive radiation in NWM

was triggered by an association of size evolution with dietary diversification (Marroig and Cheverud 2004). This association is apparent in our results here in the significant correlation between size and diet (Fig. 3). The largest NWM are leaf-eaters and the smallest are gum-eaters (Fig. 3). Tables 4 and 5 also show this relationship with size differences (s_{dif}) and morphological amount and pace of evolutionary change (m_{amount} and m_{pace}) being associated with both dietary change measures (d_{amount} and d_{pace}), suggesting that larger dietary differences are associated with larger size differences. The association of size and diet evolution is also apparent in the *t*-tests comparing the new invasion and stable groups. Significant differences were observed for size difference (s_{dif}), Δz-g_{max} and Δz-p_{max}, indicating that indeed the largest absolute size transitions are associated with the invasion of new dietary adaptive zones and that the direction of evolutionary change was close to the LLER in those invasions.

An empirical pattern found by Kay (1984) looking at the distribution frequency of primate species body sizes and diet is that dietary habits are correlated with body size (Fleagle 1999). Species that eat insects tend to be relatively small, whereas those that eat leaves tend to be relatively large (Kay 1984). But why should diet and morphological evolution, especially size, be associated? The answer involves the relationships between absolute size changes, ecological opportunity related to empty diet niches in the past, and metabolic, physiologic, and foraging issues related to scaling (for a thorough account of the ideas discussed below, see Fleagle 1999, ch. 9, and references therein). Perhaps the easiest way to visualize these relationships is to consider a simple question: Why don't we have large primates feeding predominantly on insects, or tiny vegetarian primates eating mainly tree leaves? All NWM are fruit eaters that supplement their diets with other items to meet the needs of a balanced diet in terms of energy and other nutritional requirements, such as proteins and trace elements (Fleagle 1999). Fruits are a good source of calories but are very low in protein content. To supplement their diets two abundant resources are usually exploited by primates: other animals (such as insects) and folivorous material (leaves, shoots, and buds). Insects (and animal material in general) are an excellent source of nutrients and calories per unit weight, but they are difficult to catch and the numbers of prey items ingested during an active period should be dependent on their local abundance. Small primates can live by preying on insects quite effectively but a large animal will not be able to capture enough insects to meet its needs for protein and energy. Unlike insects, leaves are neither cryptic nor difficult to catch, but instead pose other problems for their consumers. While a good source of protein, leaves are generally low in energy yield for their weight compared to fruits and insects. Consequently, large amounts must be ingested and processed by the gut. Leaves are also composed of large amounts of less digestible components, like cellulose or even toxins. A larger body helps a primate overcome these problems inherent to a leafy diet providing longer gut tubes, which allows proper digestion and detoxification. Thus, while the lower size limit of folivorous primates seems to be determined by metabolic and digestive parameters, the upper size limit of insect eaters seems to be imposed by the time to locate and catch prey

(Fleagle 1999). If we consider that at some point in the past, close to the beginning of the adaptive radiation of NWM, there were empty dietary niches available for invasion, size evolution is a consequence of adaptation to those niches. We can imagine that the empty dietary niches correspond to peaks in the adaptive landscape and ascending those peaks involves changes in absolute size. Thus, the ecological force driving NWM adaptive radiation is dietary diversification or, under a Simpsonian view of nature (Simpson 1953), the invasion and further subdivision of diet-based adaptive zones. Natural selection operated to diversify diet in NWM, allowing species to exploit previously unexplored adaptive zones (Van Valen 1971). The cranial morphological correlates of that adaptation were such that genera diverged along a cranial size dimension that is also the dimension of greatest variance within species (LLER).

Selection, Constraints, or Both?

One final question regards the role of selection versus constraints during the adaptive radiation. If size evolution resulted from selection operating to diversify diet in NWM, was the evolutionary change a result of the morphological integration patterns biasing the evolutionary divergence (Δz) in the direction of maximum additive genetic variance (g_{max}) or did selection operate directly upon both g_{max} and Δz? In other words, was the close link between g_{max} and the direction of evolution evidence of long-term genetic constraints or were both g_{max} and size under selection? Our results are surprising in revealing that the selection gradients (β) are not similar to either p_{max} (or g_{max}) or Δz values (Fig. 4). This suggests that the similarity observed between evolutionary change in NWM and the axis of maximum genetic variance (g_{max}) arises from the operation of long-term constraints. These constraints might be the result of stabilizing selection operating via a common developmental program that structure or modulate the expression of genetic and environmental variability (Marroig and Cheverud 2001). Therefore, our results so far suggest that the genetic correlation structure shapes macroevolutionary patterns by directing the evolution of mean phenotypes toward certain adaptive peaks and away from others, regardless the selection patterns operating (the constraints models in Björklund and Merilä 1994; Baker and Wilkinson 2003).

However, we also took another approach to test the adaptive model (Björklund and Merilä 1994; Baker and Wilkinson 2003). To test whether selection was operating primarily on size, we built an isometric hypothetical selection gradient (all 39 elements equal to 0.160 or $1/\sqrt{39}$). This size selection vector (β_{size}) was then multiplied by the $\mathbf{W}$ matrices to give the hypothetical evolutionary response to selection on size alone (Δz_h) for each internode in the NWM tree. We then compare those Δz_h values with the observed Δz values using vector correlations. The hypothetical and observed evolutionary responses tend to be quite similar ($\bar{X} = 0.77$, SD = 0.22; Table 3). Moreover, there is a striking similarity between the Δz-Δz_h and the Δz-p_{max} ($R = 0.988$, $P = 1 \times 10^{-15}$), indicating that selection on size alone would produce evolutionary responses along p_{max}. The exceptions are the same as those observed in Figure 2 and represent those cases

where evolution was not size based. A full exploration of these approaches would be to randomly generate a subset of allometric size selection vectors (not only isometric), apply them to the **W** matrices and then compare the **Δz** values produced with the observed ones and to a full set of responses produced from random selection vectors (not only allometric or isometric size). Because dietary diversification in primates is linked with body size changes, we expect that empty dietary adaptive zones would impact covariance patterns as a size selection gradient. Therefore, considering all the results presented here, it is perhaps not useful or possible to separate the influence of genetic patterns of covariation from the influence of natural selection on the evolution of NWM cranial diversity.

While it seems clear that NWM cranial diversification occurred primarily along the LLER, it is not clear whether that path was followed because of selection along it or because evolution was constrained to follow this path. Even though the general pattern is for evolution to follow the path of least resistance, several instances of diversification along other, distinct, morphological dimensions were also found (*Leontopithecus*, *Lagothrix*, *Chiropotes*, and *Pithecia*) indicating that constraint is not absolute in NWM. It is also clear that the path of least resistance is very conservative in the NWM, remaining consistent over 30 million years of evolutionary change. Genera that diverged in directions distinct from the LLER do not display especially distinctive patterns of within species allometry (Tables A1, A2 available online) or variance/covariance matrices (Marroig and Cheverud 2001), and thus their morphological diversification cannot be attributed to changes in constraints. Also, only 20–40% of the within-species variation is due to size (PC1). Clearly, there is substantial genetic variation in other dimensions for response to selection. Thus, it seems most likely that size was often the target of selection in NWM evolution and that cranial morphology evolved allometrically in response (Lande 1979; Zeng 1988).

ACKNOWLEDGMENTS

LITERATURE CITED

Ackermann, R. R., and J. M. Cheverud. 2000. Phenotypic covariance structure in tamarins (genus *Saguinus*): a comparison of variation patterns using matrix correlation and common principal component analysis. Am. J. Phys. Anthropol. 111:489–501.

Arnold, S. 1992. Constraints on phenotypic evolution. Am. Nat. 140:S85–S107.

Arnold, S., M. E. Pfrender, and A. G. Jones. 2001. The adaptive landscape as a conceptual bridge between micro- and macroevolution. Genetica 112/113:9–32.

Baker, R. H., and G. S. Wilkinson. 2003. Phylogenetic analysis of correlation structure in stalk-eyed flies (Diasemopsis, Diopsidae). Evolution 57:87–103.

Bégin, M., and D. A. Roff. 2003. The constancy of the **G** matrix through species divergence and the effects of quantitative genetic constraints on phenotypic evolution: a case study in crickets. Evolution 57:1107–1120.

Berg, R. L. 1960. The ecological significance of correlation pleiades. Evolution 14:171–180.

Björklund, M., and J. Merilä. 1994. Morphological differentiation in *Carduelis* finches: adaptive vs. constraint models. J. Evol. Biol. 6:359–373.

Blackith, R. E., and R. A. Reyment. 1971. Multivariate morphometrics. Academic Press, London.

Cheverud, J. M. 1995. Morphological integration in the saddle-back tamarin (*Saguinus fuscicollis*) cranium. Am. Nat. 145:63–89.

———. 1996. Quantitative genetic analysis of cranial morphology in the cotton-top (*Saguinus oedipus*) and saddle-back (*S. fuscicollis*) tamarins. J. Evol. Biol. 9:5–42.

———. 2001. A simple correction for multiple comparisons in interval mapping genome scans. Heredity 87:52–58.

Coimbra-Filho, A. F., and R. A. Mittermeier. 1981. Ecology and behavior of Neotropical primates. Vol. 1. Academia Brasileira de Ciências, Rio de Janeiro.

Fleagle, J. G. 1999. Primate adaptation and evolution. Academic Press, New York.

Garland, T., Jr.,and A. R. Ives. 2000. Using the past to predict the present: confidence intervals for regression equations in phylogenetic comparative methods. Am. Nat. 155:346–364.

Hershkovitz, P. 1977. Living New World monkeys (Platyrrhini) with an introduction to Primates. Vol. I. Univ. of Chicago Press, Chicago.

Jones, A. G., S. J. Arnold, and R. Bürger. 2004. Evolution and stability of the **G**-matrix on a landscape with a moving optimum. Evolution: 58:1639–1654.

Kay, R. F. 1984. On the use of anatomical features to infer foraging behavior in extinct primates. Pp. 21–53 *in* J. Cant and P. Rodman, eds. Adaptations for foraging in nonhuman primates. Columbia Univ. Press, New York.

Kinsey, W. G. 1997. New World primates: ecology, evolution, and behavior. Walter de Gruyter, New York.

Kumar, S., K. Tamura, I. B. Jakobsen, and M. Nei. 2001. MEGA2: Molecular evolutionary genetics analysis software. Arizona State University, Tempe, AZ.

Lande, R. 1979. Quantitative genetic analysis of multivariate evolution, applied to brain: body size allometry. Evolution 33:402–416.

Lofsvold, D. 1988. Quantitative genetics of morphological differentiation in Peromyscus. II. Analysis of selection and drift. Evolution 42:54–67.

Maddison, W. P., and D. R. Maddison. 2003. Mesquite: a modular system for evolutionary analysis. Ver. 1.0. Available via http://mesquiteproject.org.

Marroig, G., and J. M. Cheverud. 2001. A Comparison of phenotypic variation and covariation patterns and the role of phylogeny, ecology and ontogeny during cranial evolution of New World monkeys. Evolution 55:2576–2600.

———. 2004. Did natural selection or genetic drift produce the cranial diversification of Neotropical monkeys? Am. Nat. 163:417–428.

Maynard Smith, J., R. Burian, S. Kauffman, P. Alberch, J. Campbell, B. Goodwin, R. Lande, D. Raup, and L. Wolpert. 1985. Developmental constraints and evolution. Q. Rev. Biol. 60:265–287.

Mittermeier, R. A., A. B. Rylands, A. F. Coimbra-Filho, and G. A. B. Fonseca. 1988. Ecology and behavior of Neotropical primates. Vol. 2. World Wildlife Fund, Washington, DC.

Norconk, M. A., A. L. Rosenberger, and P. A. Garber. 1996. Adaptive radiations of Neotropical primates. Plenum Press, New York.

Omland, K. E. 1999. The assumptions and challenges of ancestral state reconstructions. Syst. Biol. 48:604–611.

Rosenberger, A. L., M. A. Norconk, and P. A. Garber. 1996. New perspectives on the Pitheciines. Pp. 329–333 in M. A. Norconk, A. L. Rosenberger, and P. A. Garber, eds. Adaptive radiations of Neotropical primates. Plenum Press, New York.

Rylands, A. B., H. Schneider, A. Langguth, R. A. Mittermeier, C. P. Groves, and E. Rodríguez-Luna. 2000. An assessment of the diversity of New World primates. Neotropical Primates 8:61–93.

Schneider, H. 2000. The current status of the New World monkey phylogeny. An. Acad. Bras. Ciênc. 72:165–172.

Schneider, H., and A. L. Rosenberger. 1996. Molecules, morphology, and Platyrrhini systematics. Pp. 3–19 in M. A. Norconk, A. L. Rosenberger, and P. A. Garber, eds. Adaptive radiations of Neotropical primates. Plenum Press, New York.

Schneider, H., F. C. Canavez, I. Sampaio, M. A. M. Moreira, C. H. Tagliaro, and H. N. Seuanez. 2001. Can molecular data place each neotropical monkey in its own branch? Chromosoma 109:515–523.

Schluter, D. 1996. Adaptive radiation along genetic lines of least resistance. Evolution 50:1766–1774.

———. 2002. The ecology of adaptive radiation. Oxford Univ. Press, Oxford, U.K.

Schluter, D., T. Price, A. Ø. Mooers, and D. Ludwig. 1997. Likelihood of ancestor states in adaptive radiation. Evolution 51:1699–1711.

Simpson, G. G. 1953. Major features of evolution. Columbia Univ. Press, New York.

Van Valen, L. 1971. Adaptive zones and the orders of mammals. Evolution 25:420–428.

Zeng, Z.-B. 1988. Long-term correlated response, interpopulation covariation, and interespecific allometry. Evolution 42:363–374.

Corresponding Editor: P. Wainwright